

Choosing units and coordinate systems

(Calculating Quantities)

Stuart D. Bale

University of California, Berkeley

(bale@berkeley.edu)

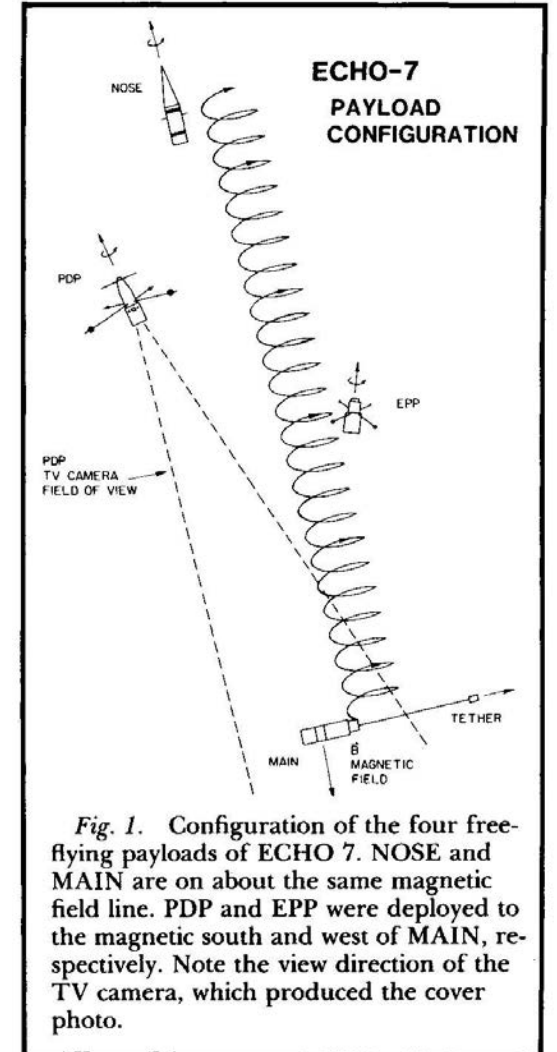
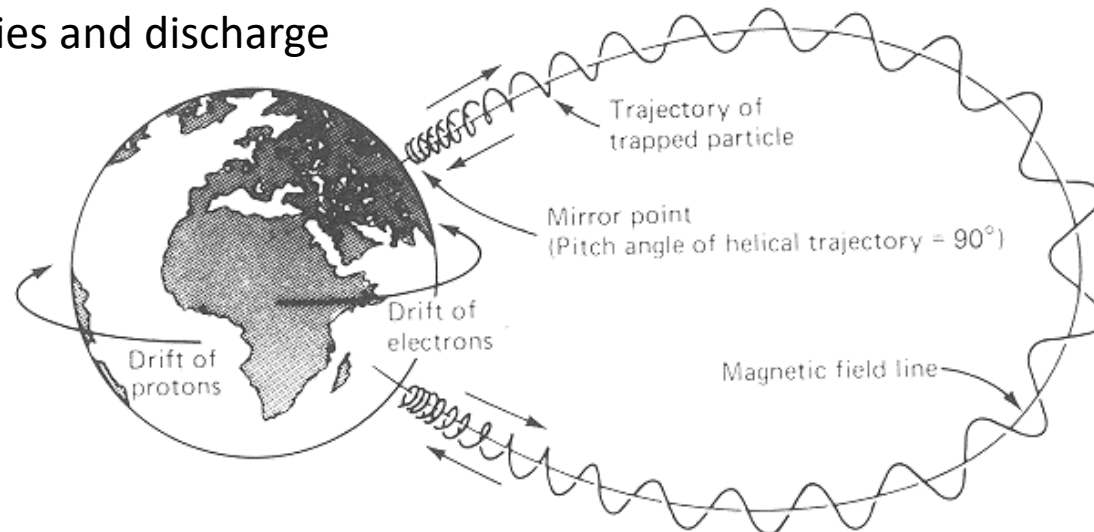
Who am I? Why am I here?

PhD work: SCEX3 and Electron Echo 7

University of Minnesota

Two separate NASA sounding rocket experiments

- Electron Echo 7
 - 35 keV electron coded pulse electron beam
 - Subpayloads with sensors
 - Measured dipole field line lengths
- SCEX 3
 - Variable (1-6 keV) coded beam
 - Subpayloads with sensors
 - Mostly measured instabilities and discharge



PhD work: Shoemaker-Levy 9

- Built up a 2-element decametric array and receiver system in Hartebeesthoek RAO in SA
- No evidence of decametric emission associated with SL-9

THE ASTROPHYSICAL JOURNAL, 484:432–438, 1997 July 20
© 1997. The American Astronomical Society. All rights reserved. Printed in U.S.A.

LIMITS ON DECAMETRIC RADIATION FROM THE SHOEMAKER-LEVY 9 IMPACTS ON JUPITER

PAUL J. KELLOGG, KEITH GOETZ, AND STEVEN J. MONSON
School of Physics and Astronomy, University of Minnesota, Minneapolis, MN 55455;
kellogg@waves.space.umn.edu; goetz@waves.space.umn.edu; monson@waves.space.umn.edu

AND

STUART D. BALE
The Astronomy Unit, Queen Mary and Westfield College, Mile End Road, London E1 4NS, England, UK;
s.d.bale@qmw.ac.uk

Received 1996 September 9; accepted 1997 February 7

ABSTRACT

Observations were carried out from South Africa (lat. = $-25^{\circ}89$, long. = $27^{\circ}69$) of the collisions of fragments A, E, H, Q1, Q2, and S with Jupiter. The excellent observing location and winter ionosphere allowed observations at important low frequencies not routinely accessible at other sites. Observations were carried out at 7.06, 8.7, 10.2, and 11.9 MHz, and in the entire band 12.4–34 MHz. No signals which could definitely be attributed to the collisions were seen. Significant upper limits on the emissions, depending on frequency and on the observing conditions during the particular impact, were obtained.

Subject headings: comets: individual (Shoemaker-Levy 9) — planets and satellites: individual (Jupiter) — radio continuum: solar system





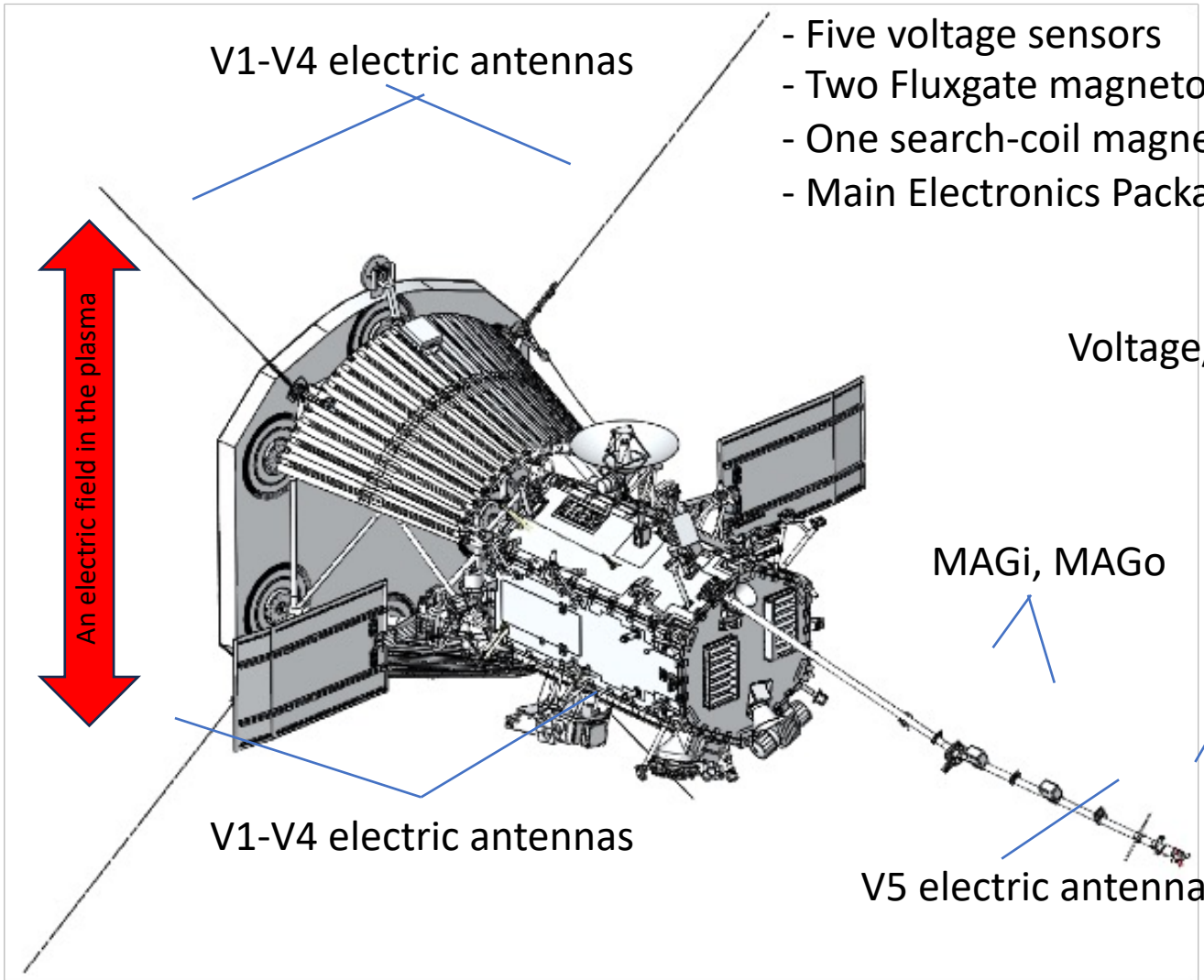
Cluster 1 mission spacecraft!



Wind spacecraft!

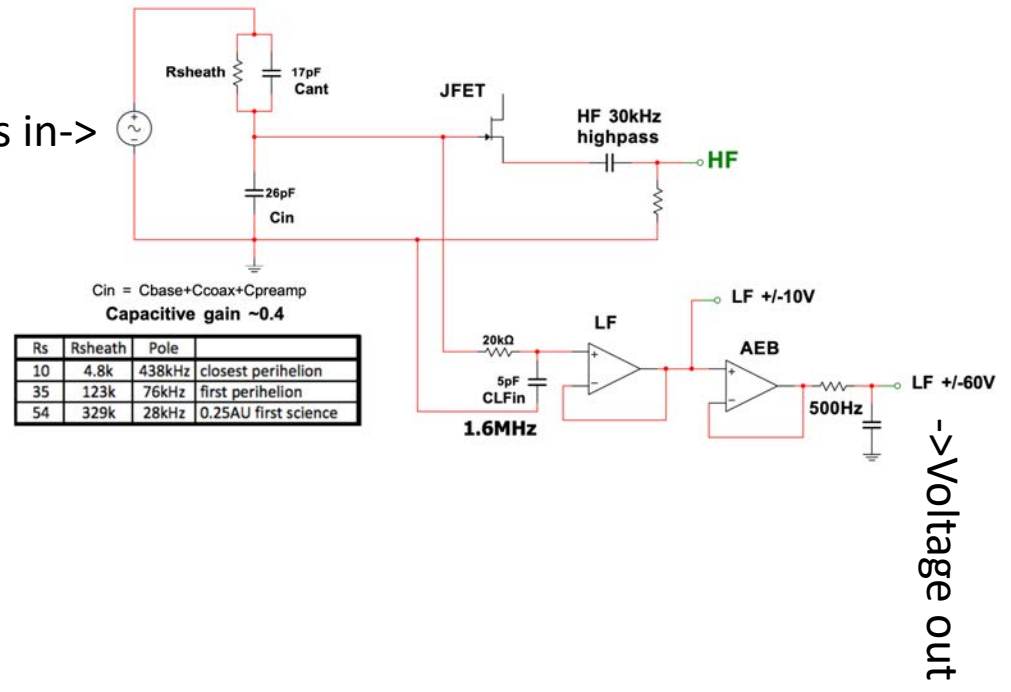
- Postdoctoral Career
 - 1994-1997 - Astronomy Unit, QMW with Steve Schwartz and David Burgess
 - Professional Career
 - 1997-2004 - Assistant Research Physicist, Space Sciences Lab, UC Berkeley
 - 2004-2006 - Assistant Professor of Physics, Physics Dept, UC Berkeley
 - 2006-2009 - Associate Professor of Physics, Physics Dept, UC Berkeley
 - 2009-date - Professor of Physics, Physics Dept, UC Berkeley
 - 2008-2018 - Director of the Space Sciences Laboratory, UC Berkeley
- NASA PI for several instruments (in flight and in development)

Choosing units and coordinate systems

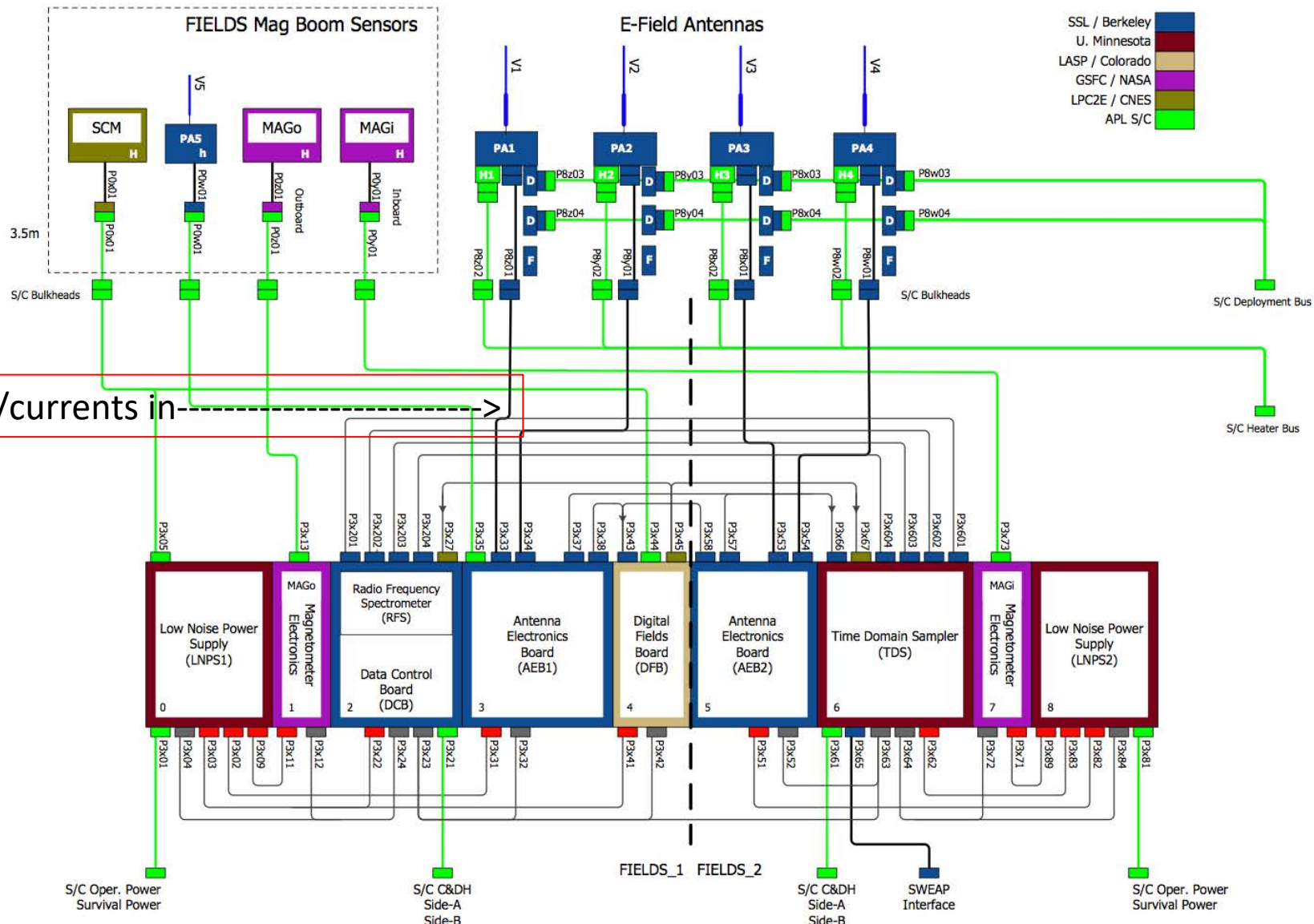


- Five voltage sensors
- Two Fluxgate magnetometers
- One search-coil magnetometer
- Main Electronics Package

Voltage/currents in->



We use 'measurements'
(Parker Solar Probe/FIELDS Instrument)



-----> numbers 01101010011 come out with clock pulses... and we use software to turn these into 'engineering' units vs time

English Engineering Units

3 languages

Contents [hide] Article Talk Read Edit View history Tools

(Top)

- Definition
- History and etymology
 - British Engineering Units
- See also
- Notes
- References

From Wikipedia, the free encyclopedia

Some fields of **engineering** in the United States use a system of measurement of physical quantities: **Engineering Units**.^{[1][2]} Despite its name, the system is based on **United States customary units** of

Definition [edit]

The English Engineering Units is a system of **consistent units** used in the United States. The set is consistent and **definitive conversions** to the **International System of Units**.^[4]

Dimension	English Engineering Unit	SI unit	Unit conversion
time	second (s)	second (s)	1 s
length	foot (ft)	metre (m)	0.3048 m
mass	pound mass (lb)	kilogram (kg)	0.45359237 kg
force	pound-force (lbf)	newton (N)	4.4482216152605 N

Electric

30 E.m.f.	E	volt	—	10 ⁸	10 ⁻⁸
31 Pot. gradient	H _e	volt/m.	—	10 ⁶	10 ⁻⁶
32 Resistance	R	ohm	—	10 ⁹	10 ⁻⁹
33 Resistivity	ρ	ohm.meter	—	10 ¹¹	10 ⁻¹¹
34 Conductance	G	mho, siemens	—	10 ⁻⁹	10 ⁹
35 Conductivity	γ	mho/m., siemens/m.	—	10 ⁻¹¹	10 ¹¹
36 Reactance	jX	ohm	—	10 ⁹	10 ⁻⁹
37 Impedance	Z	ohm ∠	—	10 ⁹	10 ⁻⁹
38 Quantity	Q	coulomb	—	10 ⁻¹	10 ¹
39 Displacement	Q	coulomb	—	10 ⁻¹	10 ¹
40 Current	I	ampere	—	10 ⁻¹	10 ¹
41 Current density	i	ampere/m. ²	—	10 ⁻⁵	10 ⁵
42 Capacitance	C	farad	—	10 ⁻⁹	10 ⁹
43 Spec. ind. capy.	ε/ε ₀	numeric	numeric	1	1

Magnetic

44 Flux	Φ	weber	maxwell	10 ⁸	10 ⁻⁸
45 Flux density	B	weber/m. ²	gauss	10 ⁴	10 ⁻⁴
46 Inductance	L	henry	—	10 ⁹	10 ⁻⁹
47 Rel. permeability	μ/μ ₀	numeric	numeric	1	1

base units, and New

TABLE 1

M.K.S. UNITS AND THEIR CORRESPONDING C.G.S. UNITS

NO.	QUANTITY	SYMBOL	M.K.S.U.	C.G.S.U.	C.G.S.U. IN ONE M.K.S.U.	M.K.S.U. IN ONE C.G.S.U.
<i>Mechanic</i>						
1	Length	L	meter	centimeter	10 ²	10 ⁻²
2	Mass	M	Kilogram	gram	10 ³	10 ⁻³
3	Time	T	second	second	1	1
4	Area	S	m. ²	cm. ²	10 ⁴	10 ⁻⁴
5	Volume	V	m. ³	cm. ³	10 ⁶	10 ⁻⁶
6	Frequency	f	hertz, cy./sec.	cy./sec., hertz	1	1
7	Density	d	kg./m. ³	g./cm. ³	10 ⁻³	10 ³
8	Specific gravity		numeric	numeric	1	1
9	Velocity	v	m./sec.	cm./sec.	10 ²	10 ⁻²
10	Slowness		sec./m.	sec./cm.	10 ⁻²	10 ²
11	Acceleration	a	m./sec. ²	cm./sec. ²	10 ²	10 ⁻²
12	Force	F	joule/m.	dyne	10 ⁶	10 ⁻⁶
13	Pressure	p	joule/m. ³	barye	10	10 ⁻¹
14	Angle	α, β	radian	radian	1	1
15	Ang. velocity	ω	rad./sec.	rad./sec.	1	1
16	Torque	τ	joule/radian	dyne ⊥ cm.	10 ⁷	10 ⁻⁷
17	Moment of inertia	J	kg. m. ²	g. cm. ²	10 ⁷	10 ⁻⁷

These units are great for exchanging information between humans about human-made stuff. But they are made up by us. Nature knows (almost) nothing about them.

Plasma physics units!

Cyclotron frequency

$$\omega_{ce} = \frac{eB}{m_e}$$

Plasma frequency

$$\omega_{pe} = \sqrt{\frac{ne^2}{m_e \epsilon_0}}$$

'Collision' frequency

$$\nu \propto \frac{n \log \Lambda}{T^{3/2}}$$

Knudsen number

Mach numbers

Sound speed

$$c_s = \sqrt{\frac{k_b T_e}{m_i}}$$

Thermal speed

$$v_{th,s} = \sqrt{\frac{k_b T_s}{m_s}}$$

Alfven speed

$$v_A = \frac{B}{\sqrt{\mu_0 n m_i}}$$

Debye length

$$\lambda_D = \sqrt{\frac{\epsilon_0 k_b T_e}{n_e e^2}}$$

Collisional MFP

$$\lambda_{mfp,s} = \frac{v_{th,s}}{\nu_s}$$

Inertial lengths

$$\rho_{p,s} = c / \omega_{p,s}$$

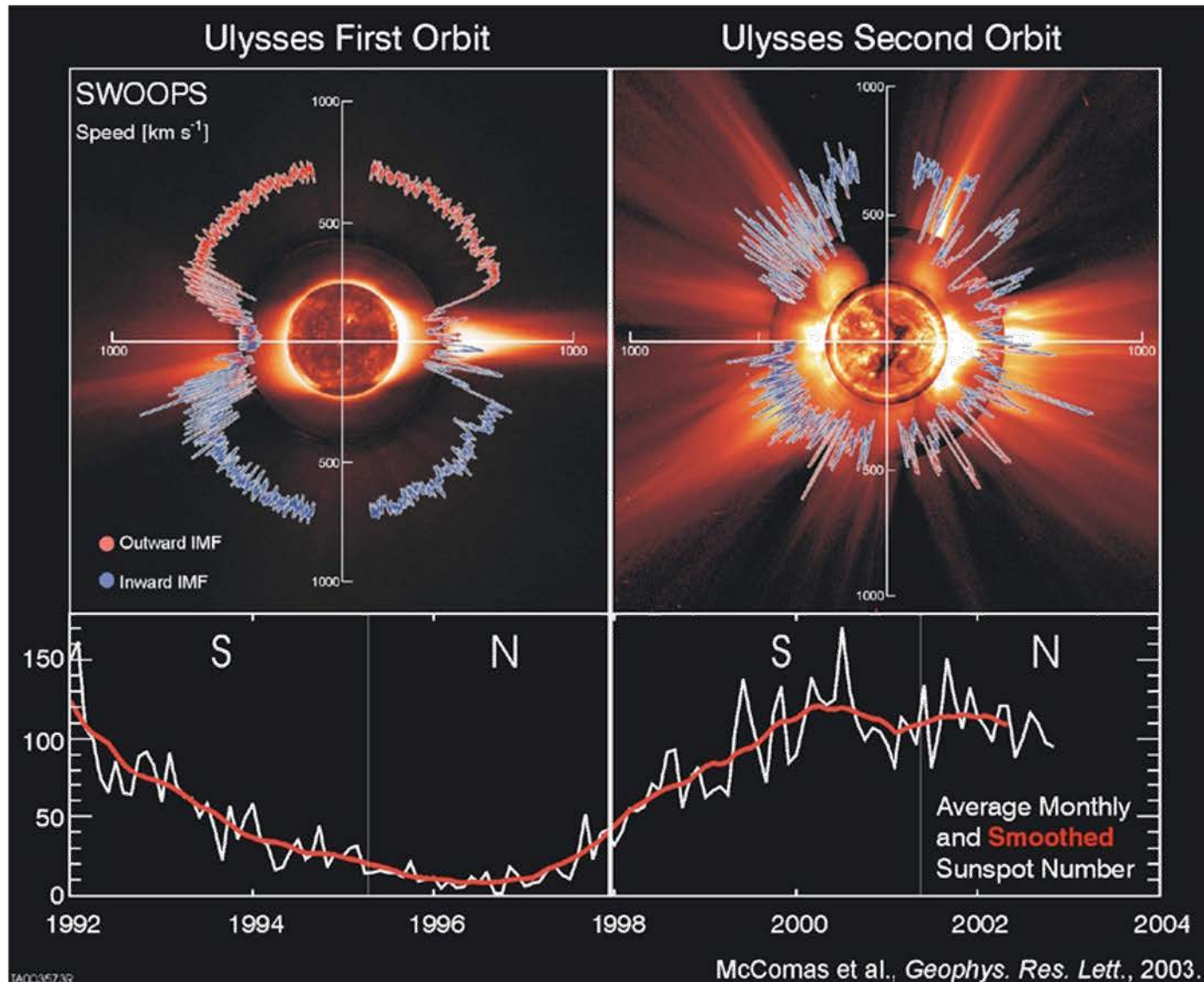
Gyroradii

$$\rho_{c,s} = v_{th,s} / \omega_{c,s}$$

Plasma beta

$$\beta_s = \frac{n_s k_b T_s}{B^2 / 2\mu_0}$$

Solar wind speed is bimodal



Fast wind (1 AU)

$V_{sw} \sim 500-1000$ km/s
 $T_p \sim 10-20$ eV
 $T_e \sim 5-20$ eV
 $n \sim 1-10$ cm⁻³
 $B \sim 5$ nT, δB is larger
 $\beta \sim 1$

Slow wind (1 AU)

$V_{sw} \sim 250-500$ km/s
 $T_p \sim 5-20$ eV
 $T_e \sim 5-20$ eV
 $n \sim 5-25$ cm⁻³
 $B \sim 5$ nT
 $\beta \sim 1$

Fast wind emerges from **coronal holes**,
Slow wind from **streamer belt (?)**

(McComas et al.)

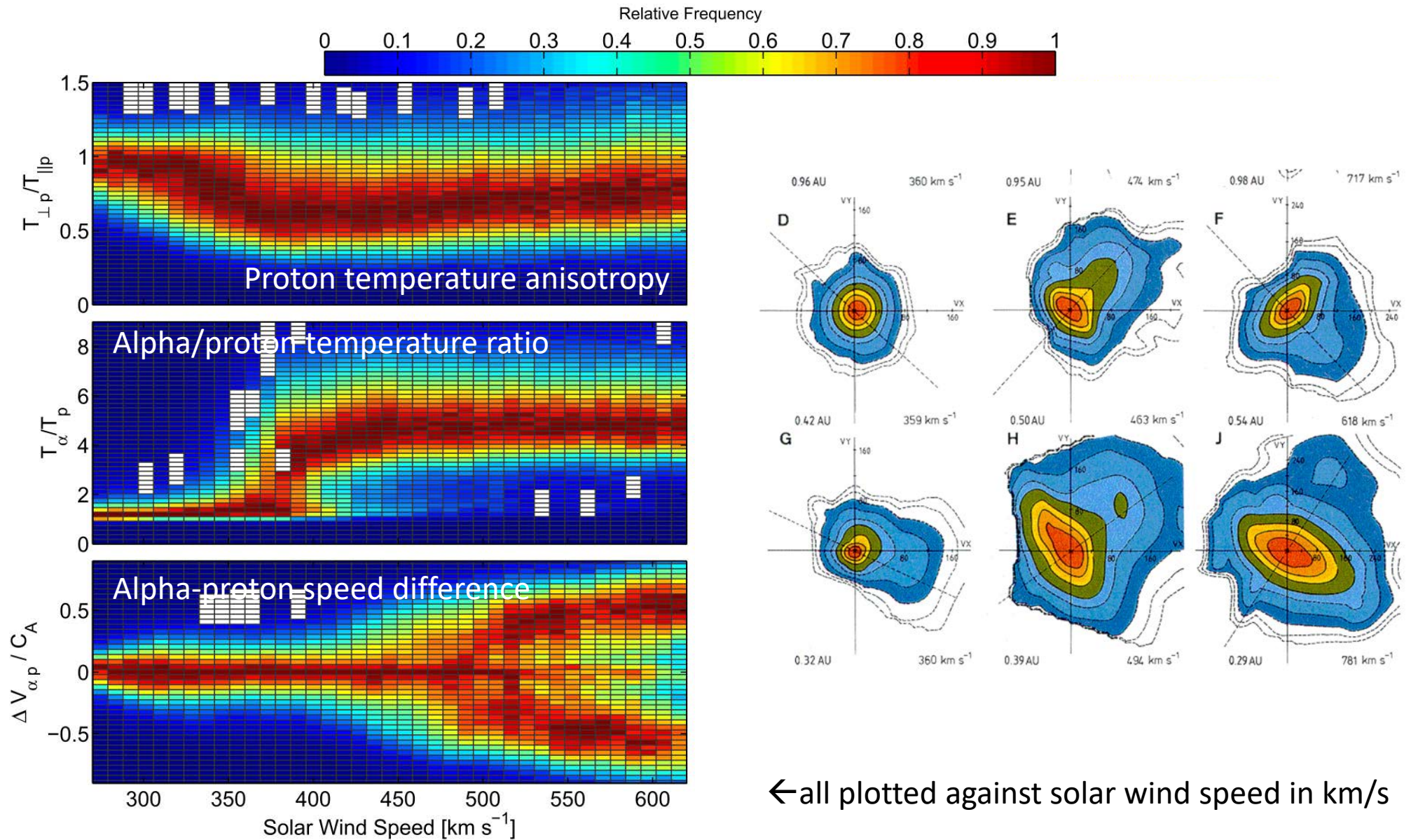


Figure 1. Two-dimensional histograms of the distributions of $T_{\perp p} / T_{\parallel p}$, T_{α} / T_p , and $\Delta V_{\alpha p} / C_A$ as functions of solar wind speed U (left) and Coulomb number N_C (right). While nonthermal solar wind is generally associated with high speeds, these distributions suggest that the occurrence frequency is really determined by the Coulomb number N_C .

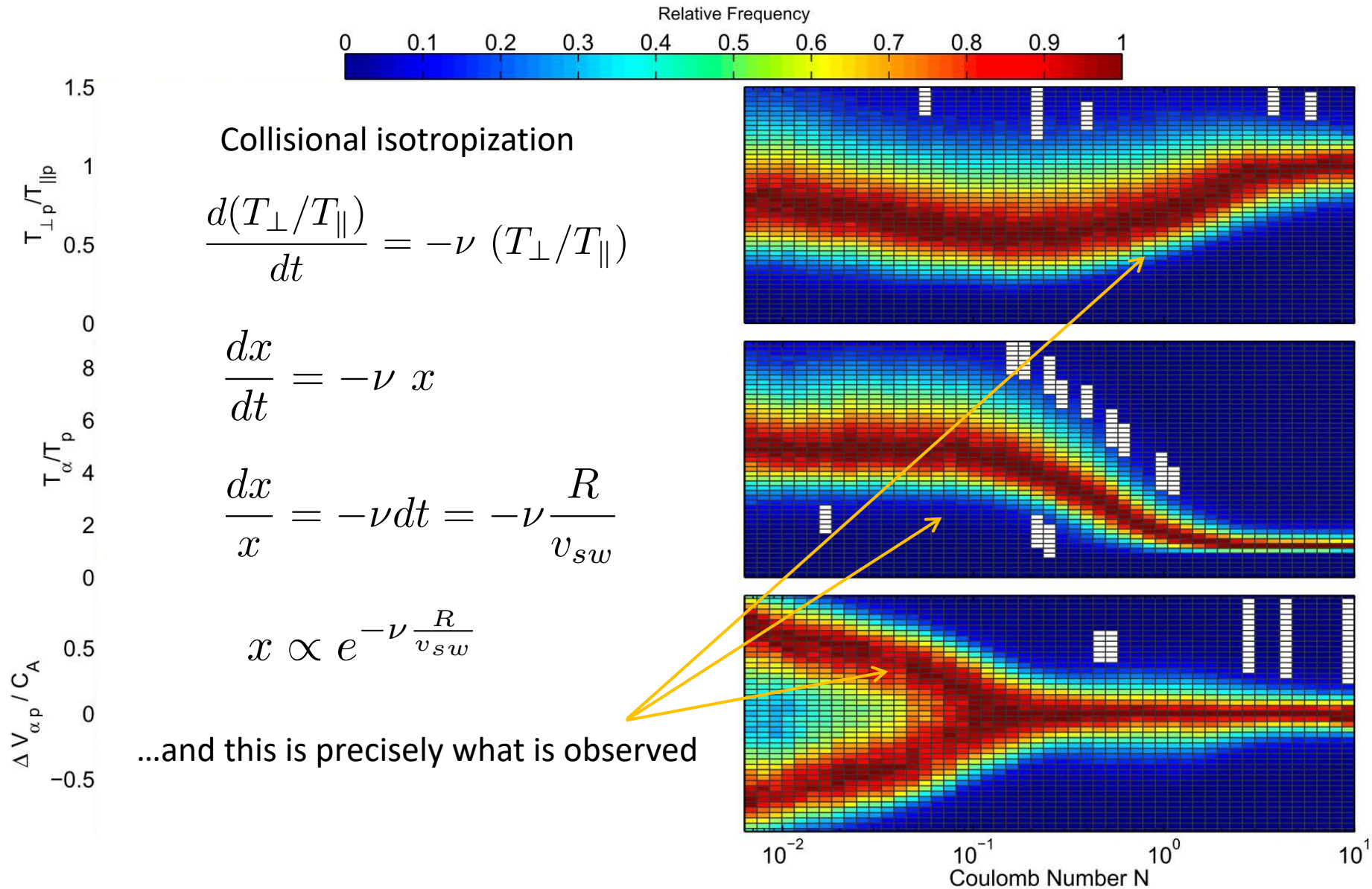


Figure 1. Two-dimensional histograms of the distributions of $T_{\perp p}/T_{\parallel p}$, T_{α}/T_p , and $\Delta V_{\alpha p}/C_A$ as functions of solar wind speed U (left) and Coulomb number N_C (right). While nonthermal solar wind is generally associated with high speeds, these distributions suggest that the occurrence frequency is really determined by the Coulomb number N_C .

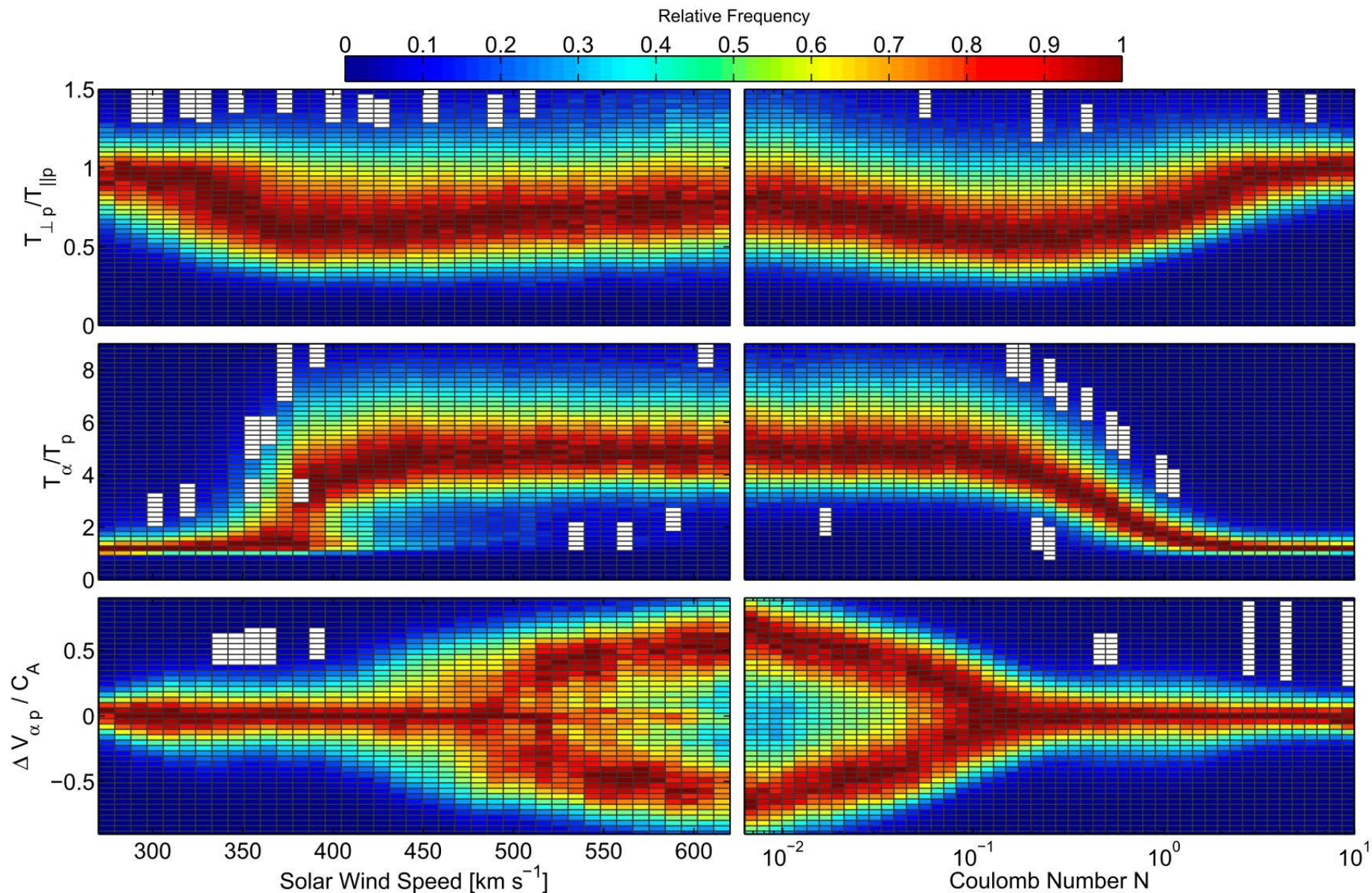
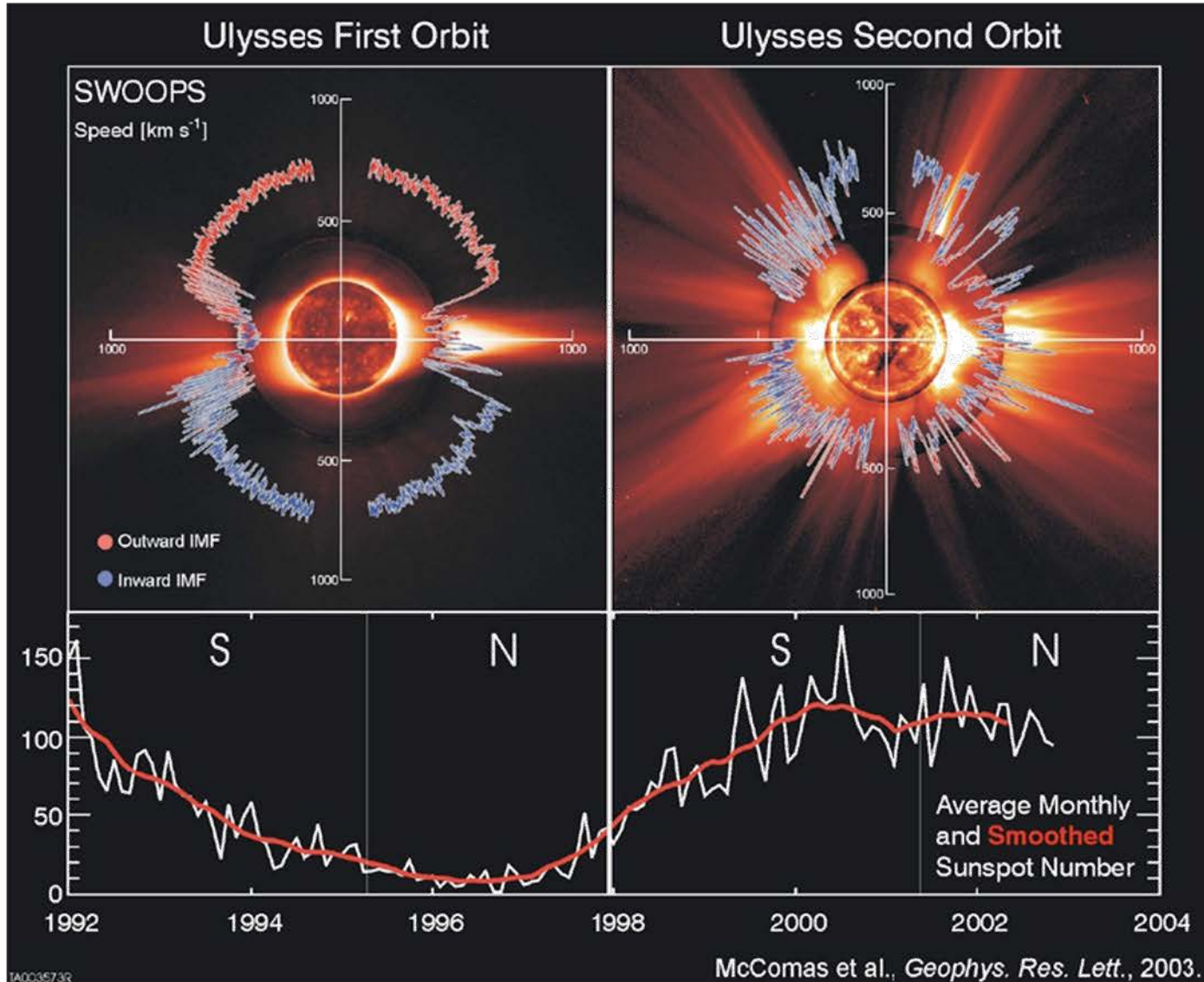


Figure 1. Two-dimensional histograms of the distributions of $T_{\perp p}/T_{\parallel p}$, T_{α}/T_p , and $\Delta V_{\alpha p}/C_A$ as functions of solar wind speed U (left) and Coulomb number N_C (right). While nonthermal solar wind is generally associated with high speeds, these distributions suggest that the occurrence frequency is really determined by the Coulomb number N_C .

Solar wind speed is bimodal



Fast wind (1 AU)

$V_{sw} \sim 500-1000 \text{ km/s}$
 $T_p \sim 10-20 \text{ eV}$
 $T_e \sim 5-20 \text{ eV}$
 $n \sim 1-10 \text{ cm}^{-3}$
 $B \sim 5 \text{ nT}, \delta B \text{ is larger}$
 $\beta \sim 1$

Slow wind (1 AU)

$V_{sw} \sim 250-500 \text{ km/s}$
 $T_p \sim 5-20 \text{ eV}$
 $T_e \sim 5-20 \text{ eV}$
 $n \sim 5-25 \text{ cm}^{-3}$
 $B \sim 5 \text{ nT}$
 $\beta \sim 1$

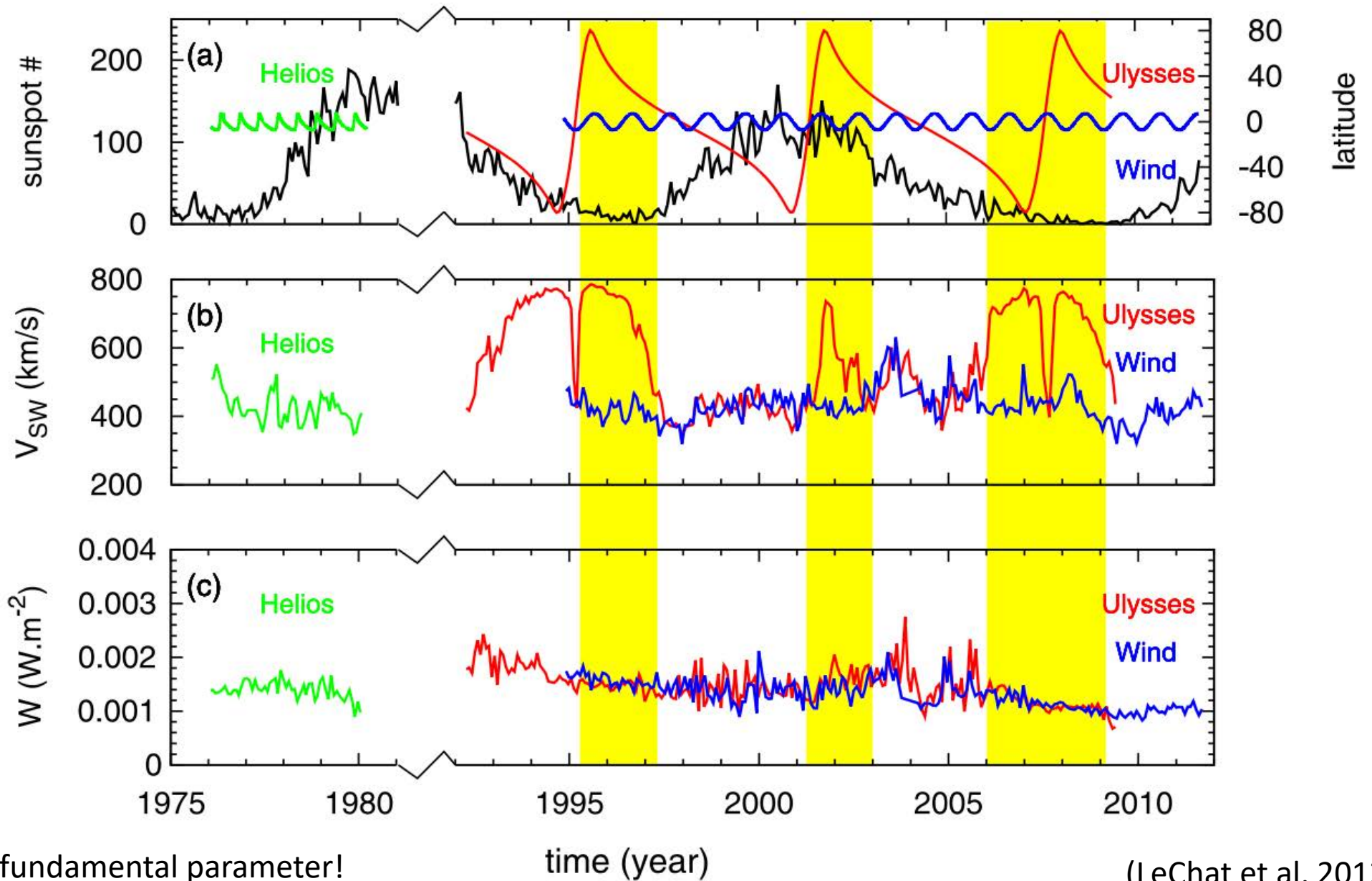
Fast wind emerges from **coronal holes**,
Slow wind from **streamer belt (?)**

(McComas et al.)

Spacecraft HG latitude
Wind, Ulysses,
Helios

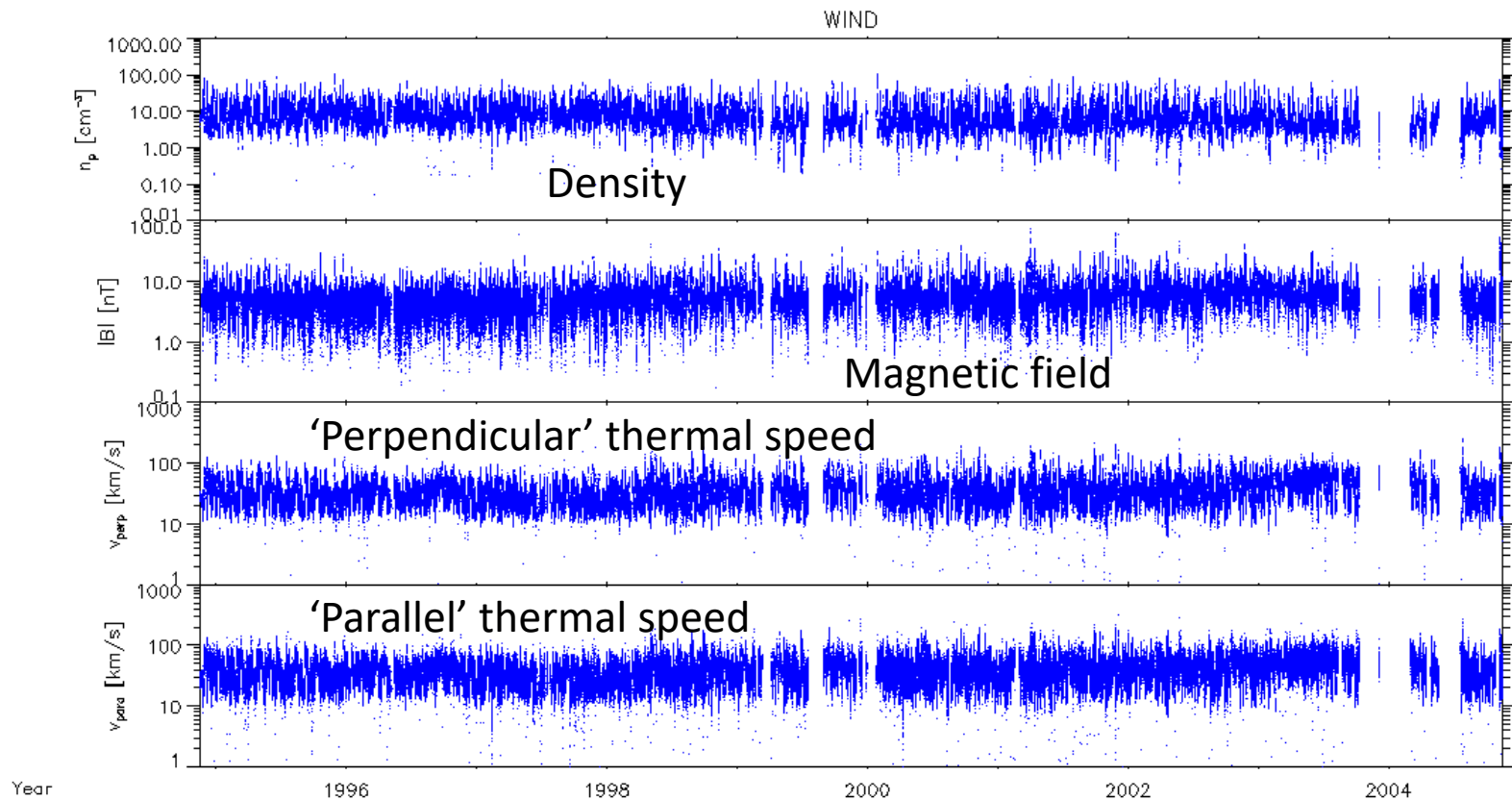
Solar wind speed
Wind, Ulysses,
Helios

Total energy flux (!)
Wind, Ulysses,
Helios



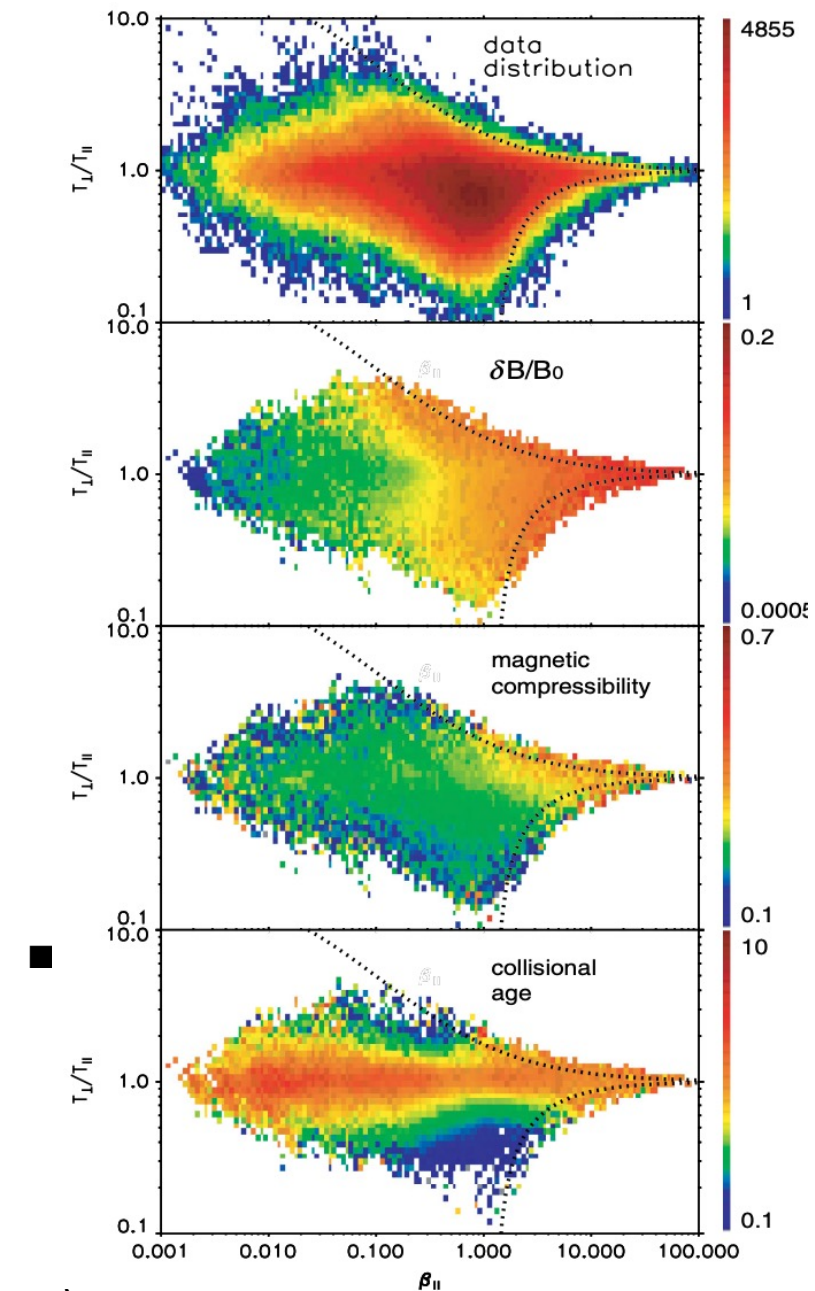
Energy flux is the fundamental parameter!

(LeChat et al, 2012)



Several years of Wind spacecraft measurements in the ambient solar wind

- entirely unremarkable as a time series
- when organized as temperature anisotropy vs plasma beta reveals the presence of *two fundamental instabilities* being excited by solar wind expansion – a new energy pathway in turbulence



(Hellinger et al., 2006; Bale et al., 2009)

Summary:

- Choose your data analysis variables based on the *physics* at hand, not simply on what's available out of the box
- Think carefully about how to create composite variables, merge datasets, etc.
 - Best cadences
 - Spectral filters and downsampling
 - Median/mode filters
 - When you become an instrument PI, be pushy about this...

Coordinate systems

- Choose your coordinate system based on the *physics* at hand, not simply on what's available out of the box
- Measurements start out in 'instrument' coordinates and are usually given to us in some simple system
 - Geocentric Solar Ecliptic (GSE)
 - Geocentric Solar Magnetic (GSM)
 - RTN

'Foreshock Coordinates'

VOL. 6, NO. 5

GEOPHYSICAL RESEARCH LETTERS

MAY 1979

THIN SHEETS OF ENERGETIC ELECTRONS UPSTREAM FROM THE EARTH'S BOW SHOCK

K. A. Anderson, R. P. Lin, F. Martel
Space Sciences Laboratory, University of California, Berkeley, CA 94720

C. S. Lin and G. K. Parks
Geophysics Program, University of Washington, Seattle, WA 98105

H. Réme
Université Paul Sabatier, Toulouse, France

VOL. 84, NO. A4

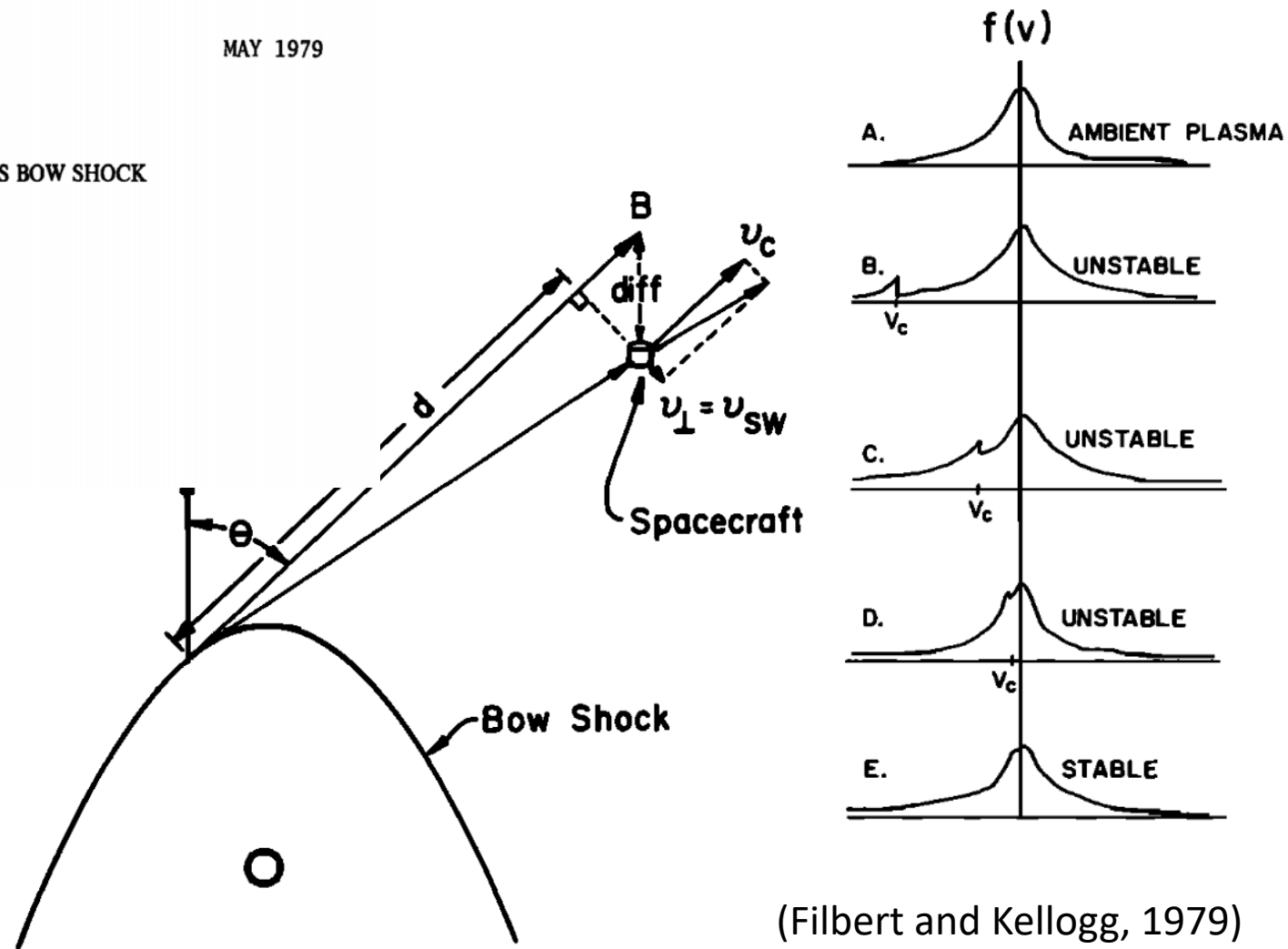
JOURNAL OF GEOPHYSICAL RESEARCH

ELECTROSTATIC NOISE AT THE PLASMA FREQUENCY

BEYOND THE EARTH'S BOW SHOCK

Paul C. Filbert and Paul J. Kellogg

School of Physics and Astronomy, University of Minnesota, Minneapolis



(Filbert and Kellogg, 1979)

Fig. 9. Geometry of the electron velocity distribution.

Distribution of electron-beam excited waves upstream of the bow shock in 'Foreshock' coordinates

702

Y. Kasaba *et al.*

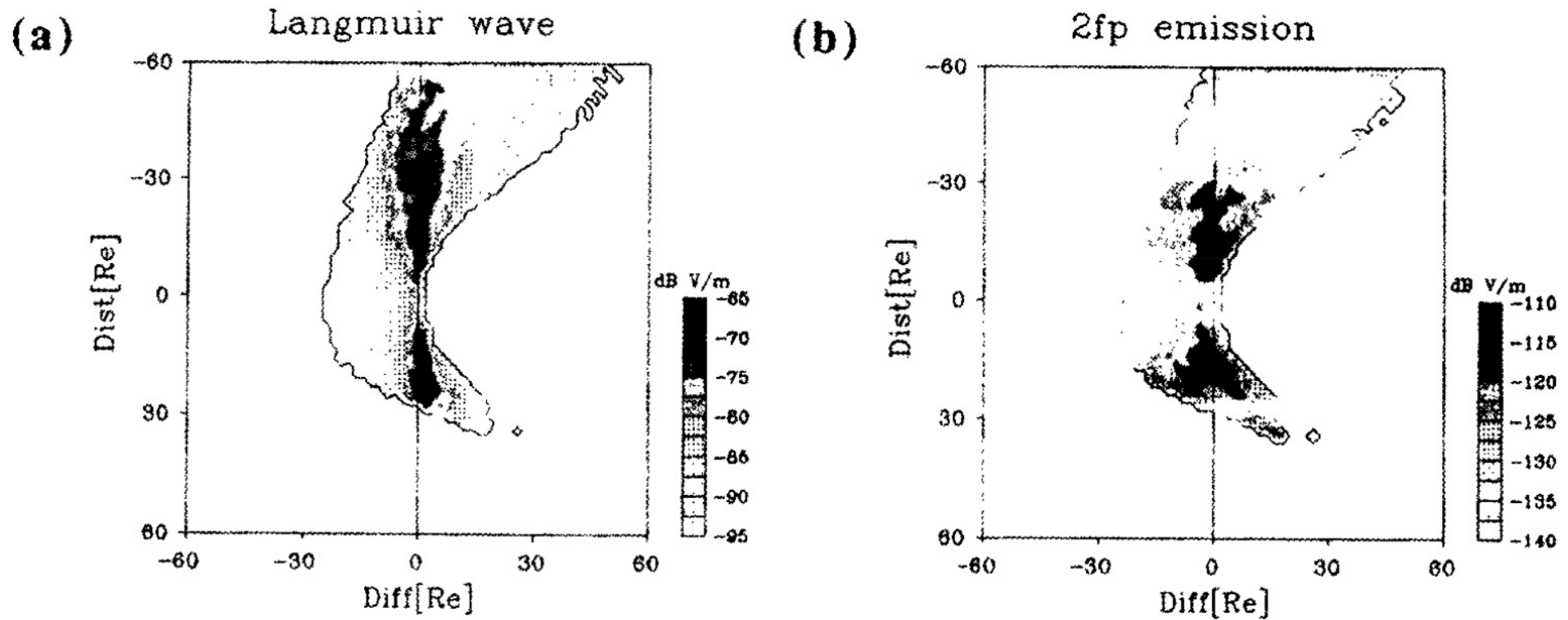


Fig. 4. Spatial distribution of (a) Langmuir waves and (b) $2f_p$ emissions on '*Diff-Dist*' coordinates

Minimum variance systems

Simple example of Principal Component Analysis (PCA) for a 3-vector (vs time)

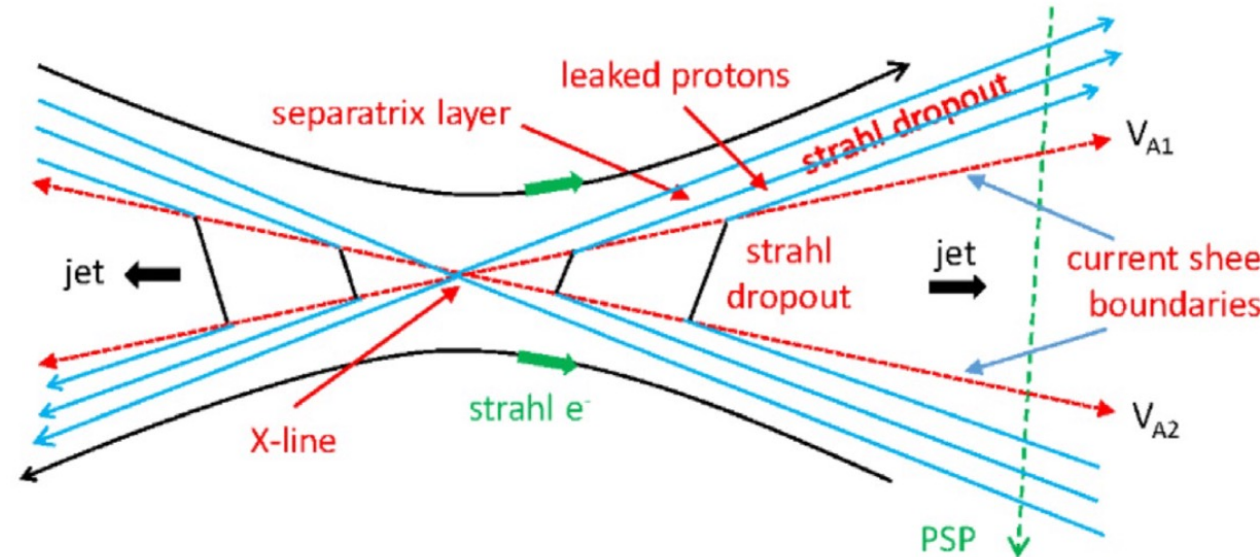
Find a unit vector \hat{n} that minimizes

$$\sigma^2 = \frac{1}{N} \sum_{i=0}^N |(\vec{B}^{(i)} - \langle \vec{B} \rangle) \cdot \hat{n}|^2$$

...gives a *rotation matrix*

$$M_{i,j} = \langle B_i B_j \rangle - \langle B_i \rangle \langle B_j \rangle$$

whose eigenvectors are unit vectors corresponding to the minimum, intermediate, and maximum variance directions.

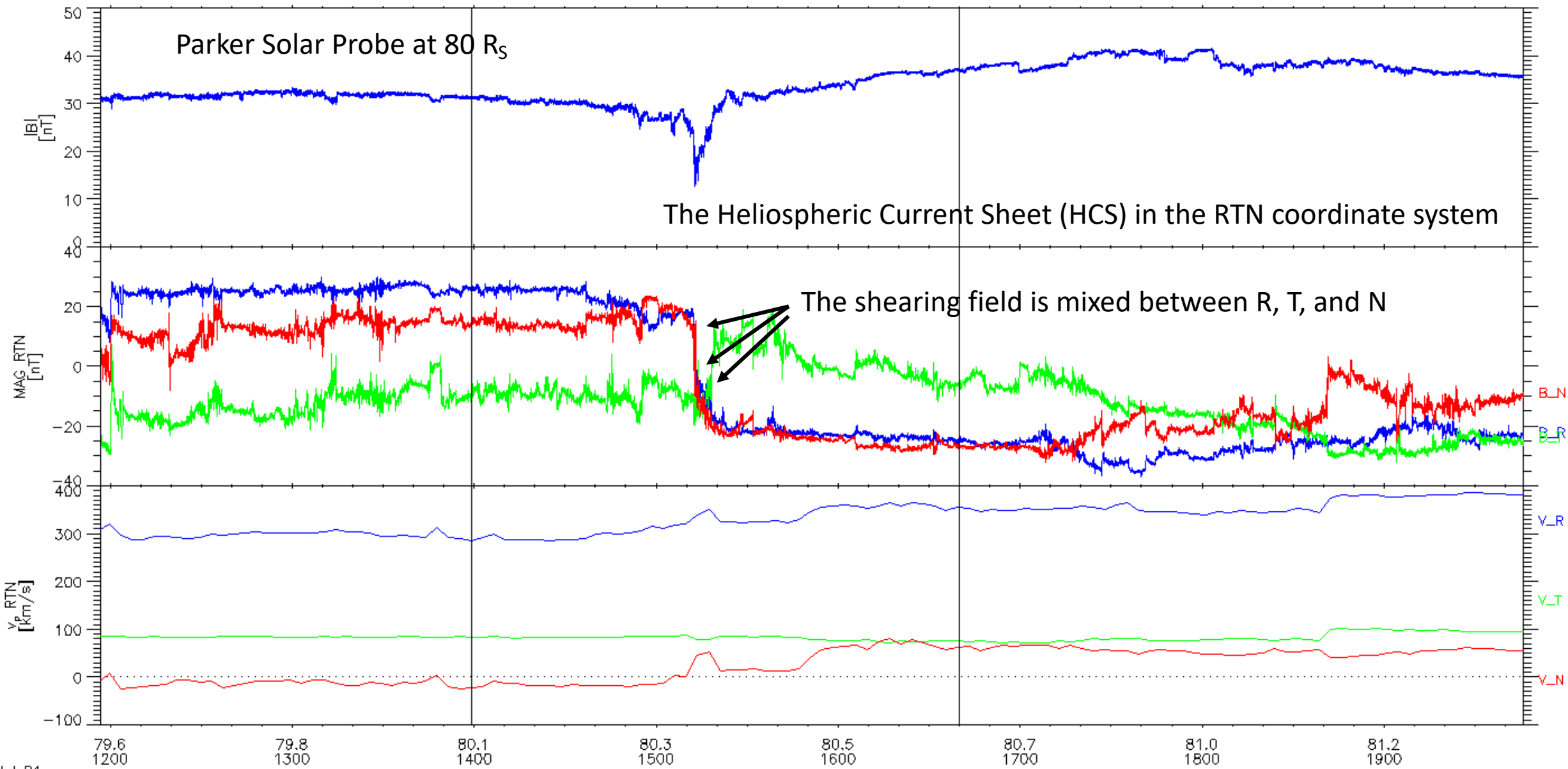


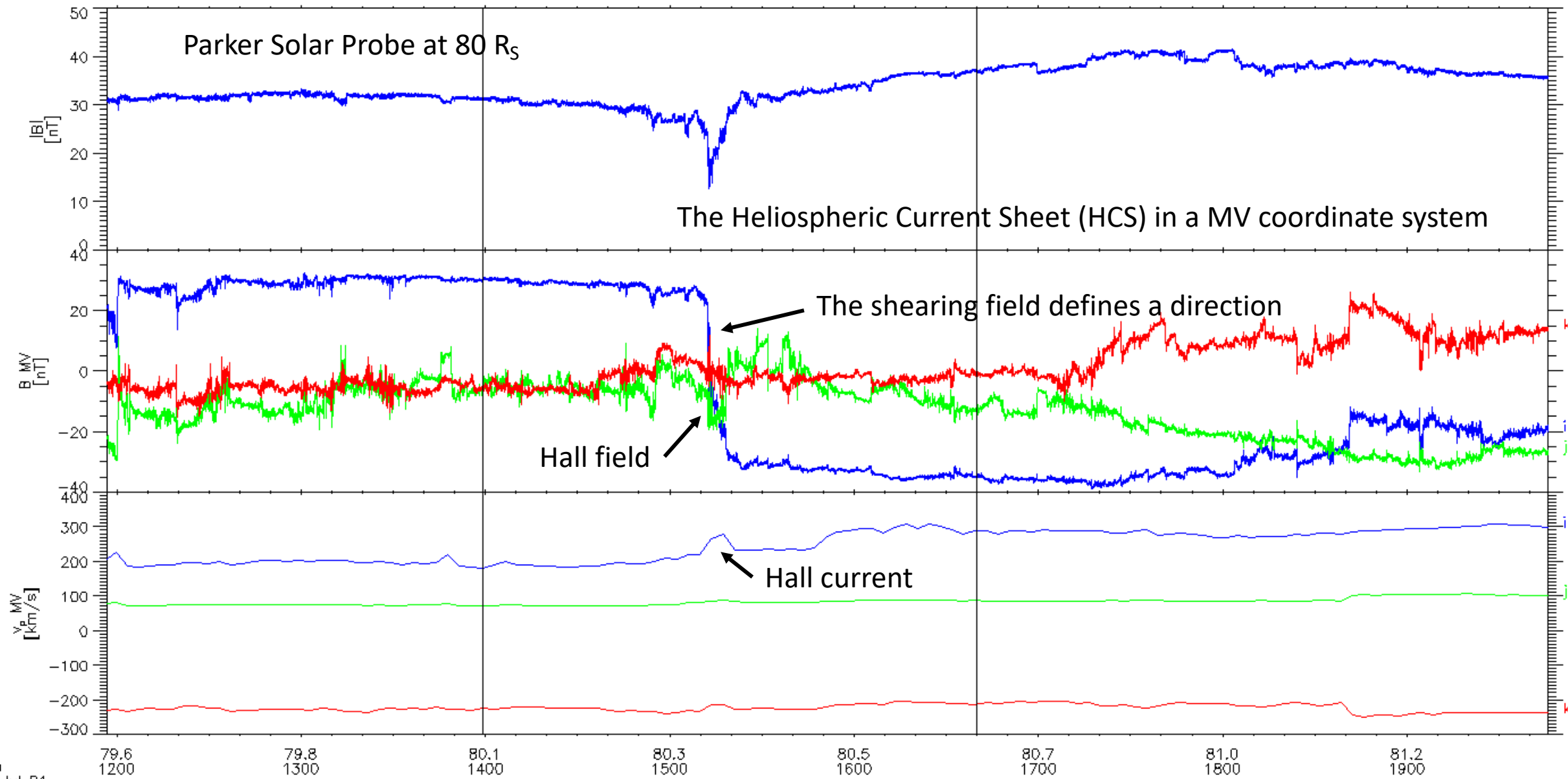
Simple current sheet geometry and divergence-free magnetic field

$$\vec{\nabla} \cdot \vec{B} = 0$$

(also nice for shocks and other boundaries)

There are more sophisticated versions of this: PCA, Faraday residue, deHoffman-Teller frames, etc.





'Carrington Coordinates'

Sun-centered, heliographic coordinate system

Fixed on the solar surface, rotating (sidereal) from an inertial frame POV

Parker Solar Probe (PSP) trajectories in inertial coordinate system

Parker Solar Probe (PSP) trajectories in Carrington coordinate system

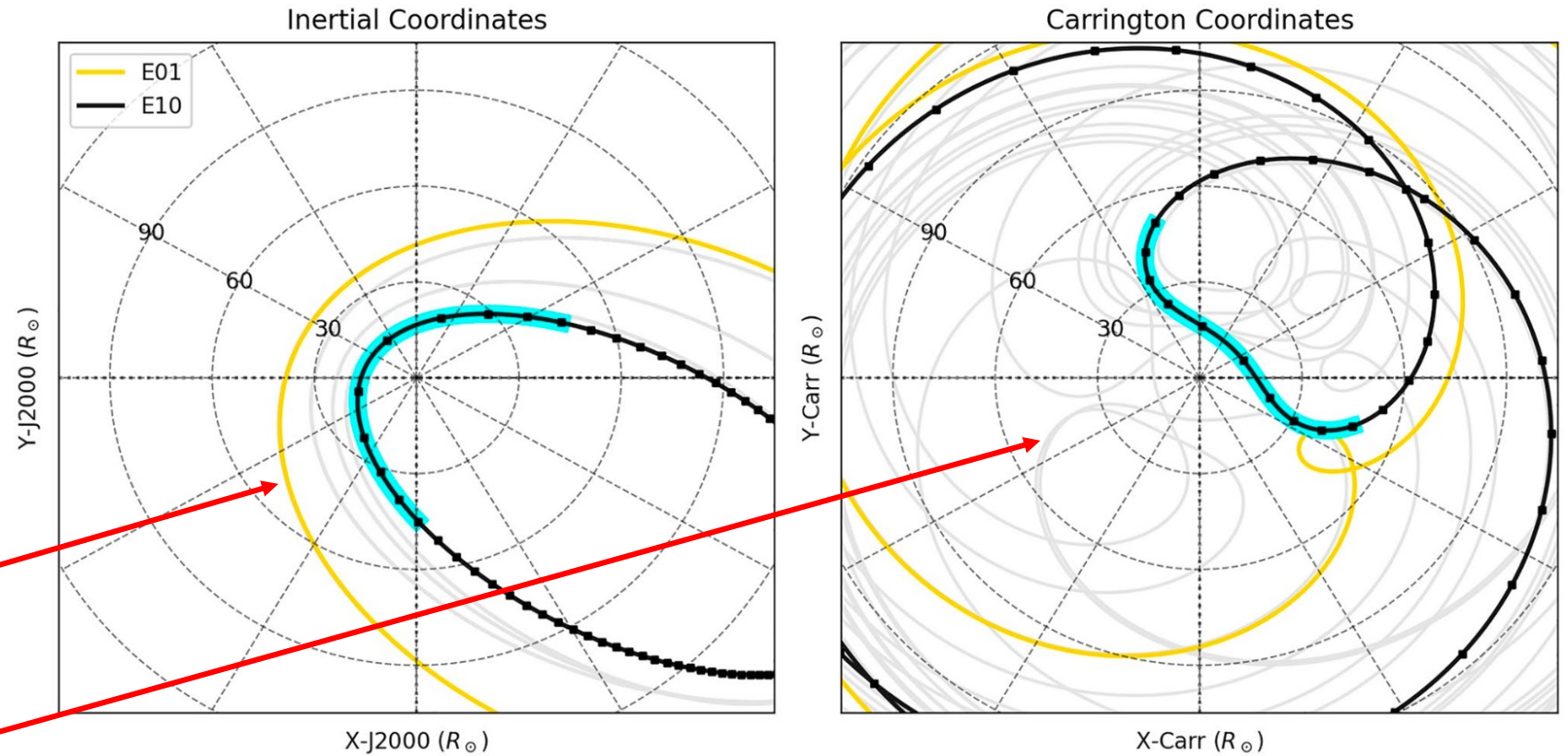
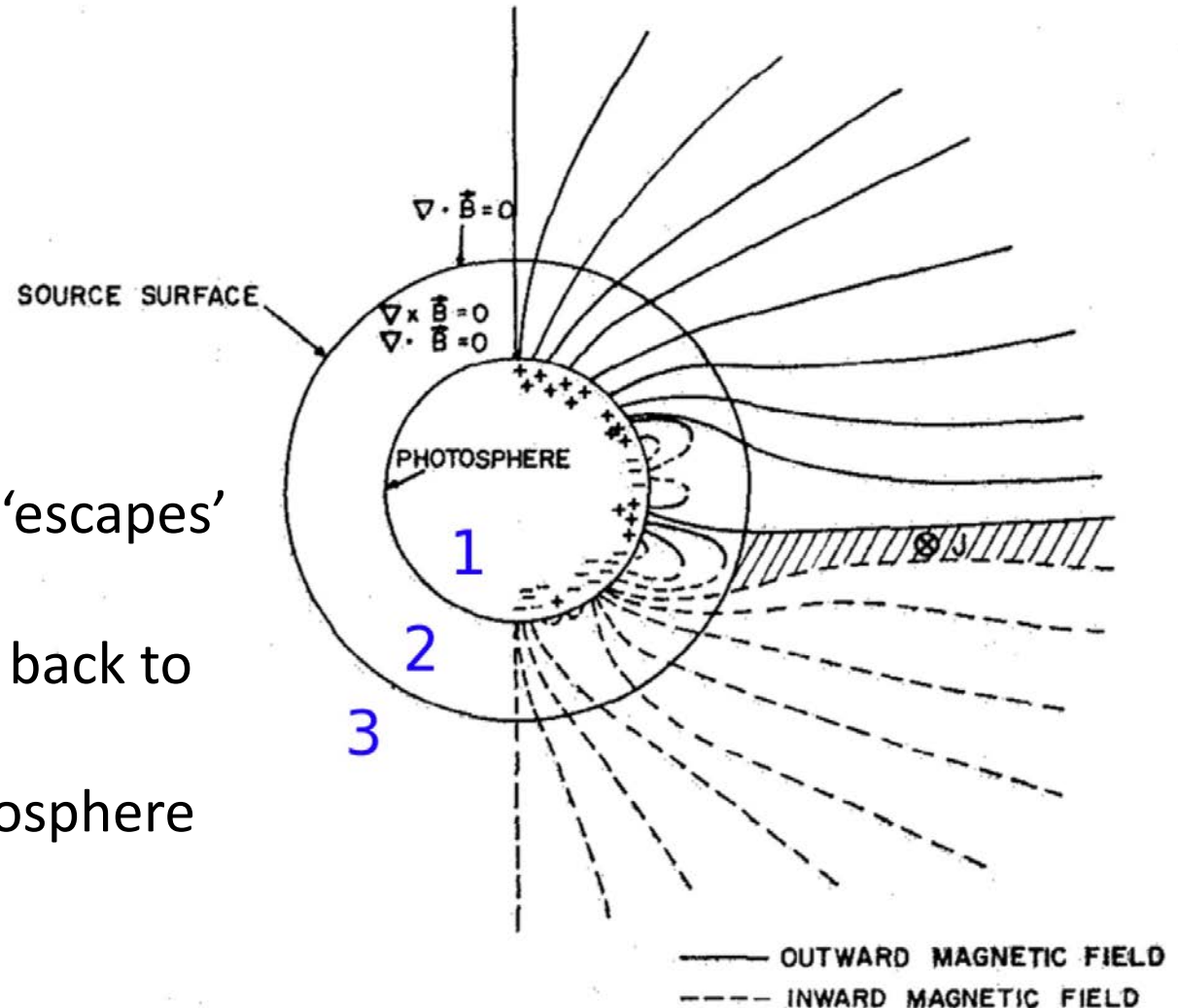


Figure 1. Orbital Geometry of the $13.3 R_{\odot}$ orbit family. Parker's E10 orbital track projected into the solar equatorial plane is shown in black with E01 shown in yellow for contrast. Black squares are spaced 24 hr apart. Faint gray curves show the full prime mission trajectory (i.e., 24 orbits). The left-hand panel shows the inertial J2000 reference frame for which the orbit's elliptical nature and decreasing perihelion is clear. The right-hand panel shows the Carrington frame, which is most relevant for source mapping. This frame demonstrates the enormous range of solar longitude traversed by Parker in its latter orbits over just a few days around perihelion. Cyan shading shows the ~ 9 -day interval of E10 where Parker co-rotates or super-rotates with respect to the Sun, which is the focus of this study.

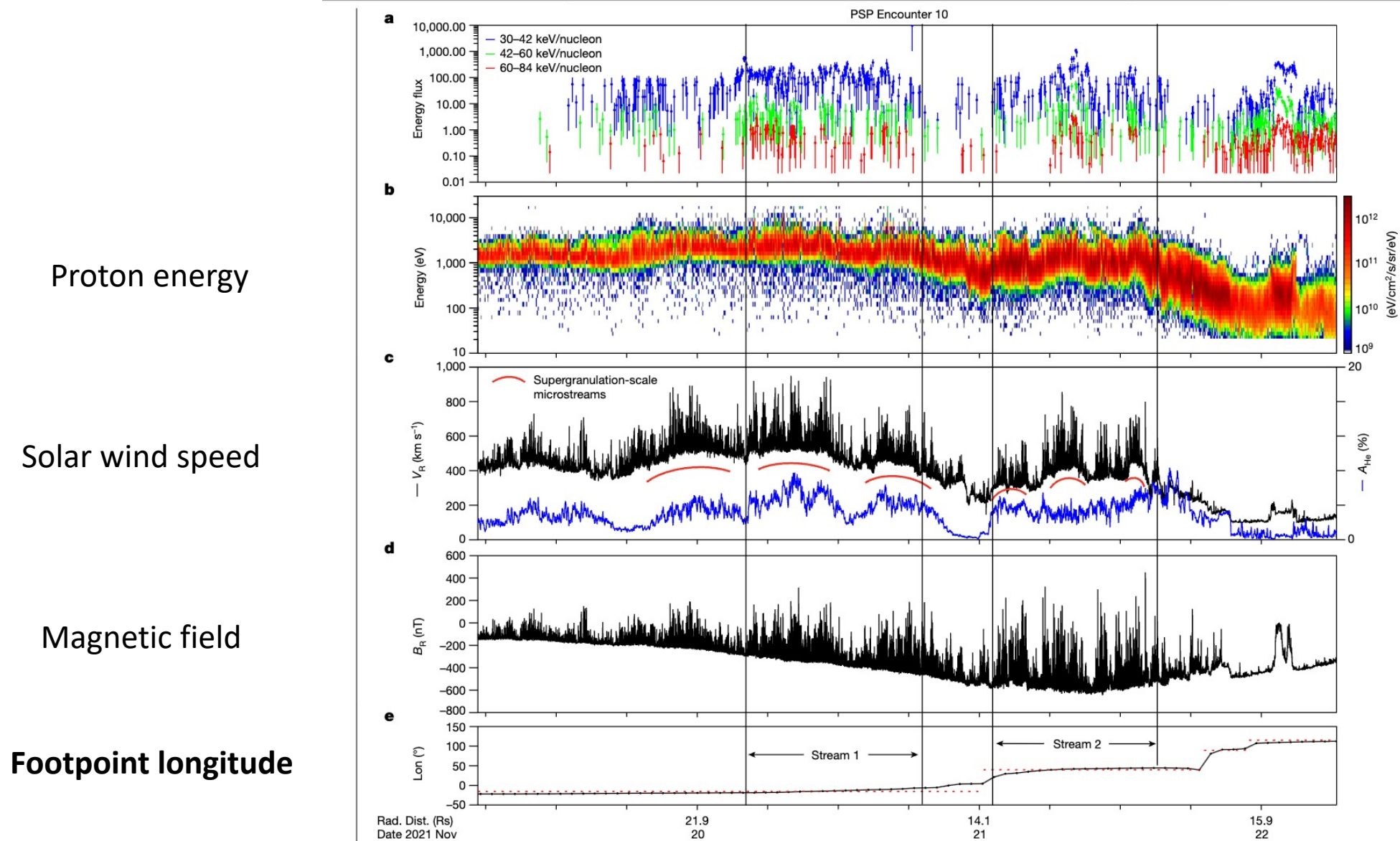
(Badman et al., 2023)

Potential Field Source Surface (PFSS) Models

- Current-free model
- Steady state
- Inner boundary condition (1/2)
 - Magnetogram data
- Outer boundary condition (2/3)
- 'Source Surface'
 - Radius from which solar wind 'escapes'
- Ballistic propagation from PSP/SO back to Source Surface
- PFSS from Source Surface to photosphere

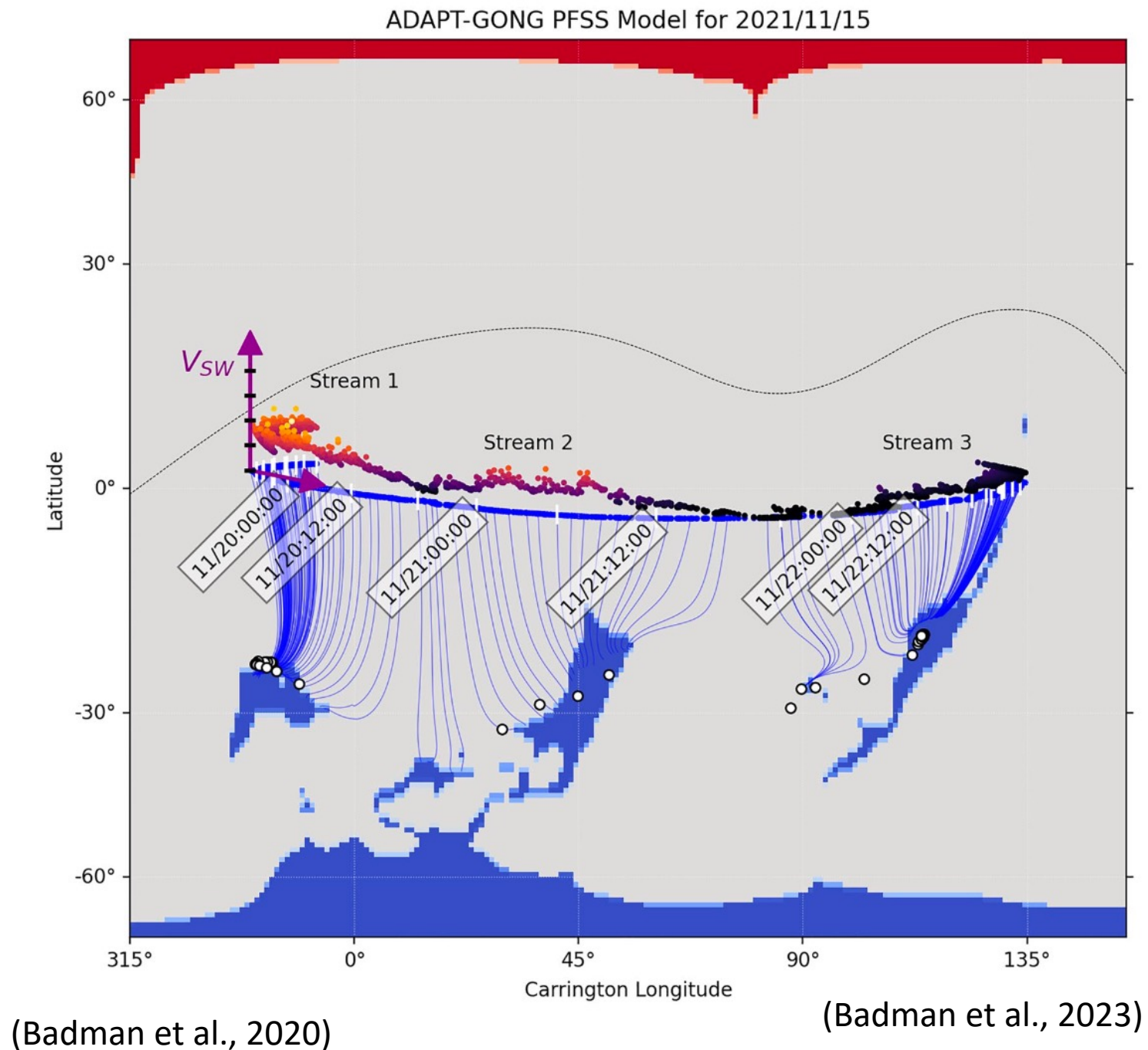
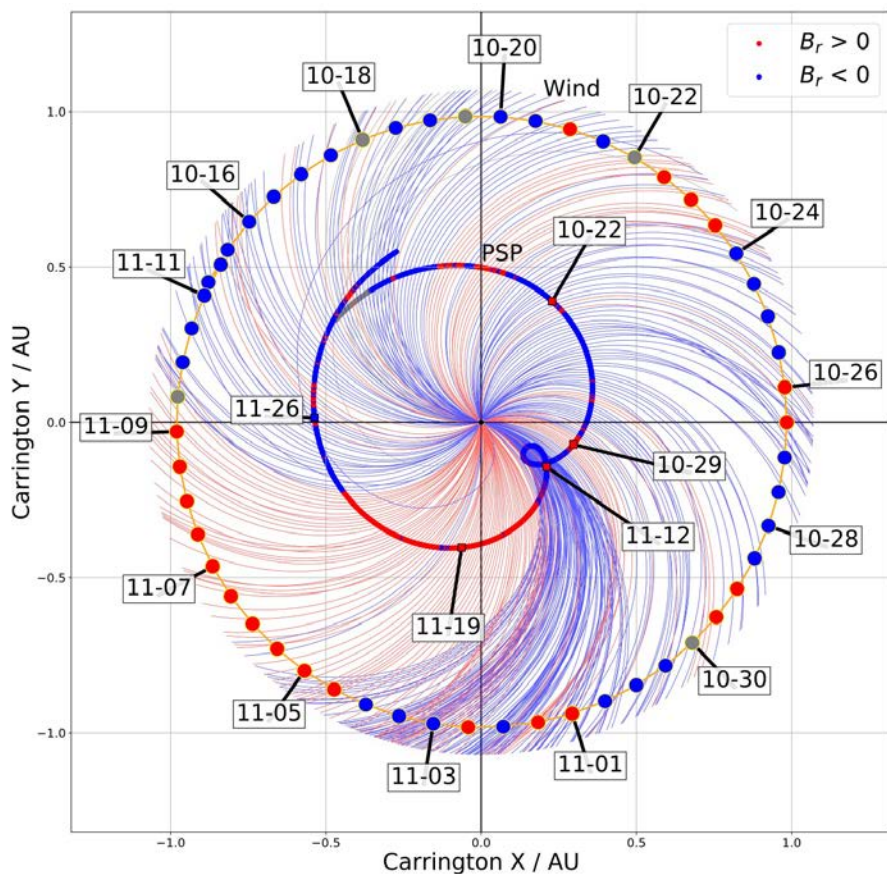


Time series data from Parker Solar Probe



PFSS/Ballistic Footpoint mapping

- Identify distinct coronal hole sources for solar wind streams



Now with 2 spacecraft - Parker Solar Probe and Solar Orbiter data – time series

SO - Charge state ratios

Density * R²

Velocity

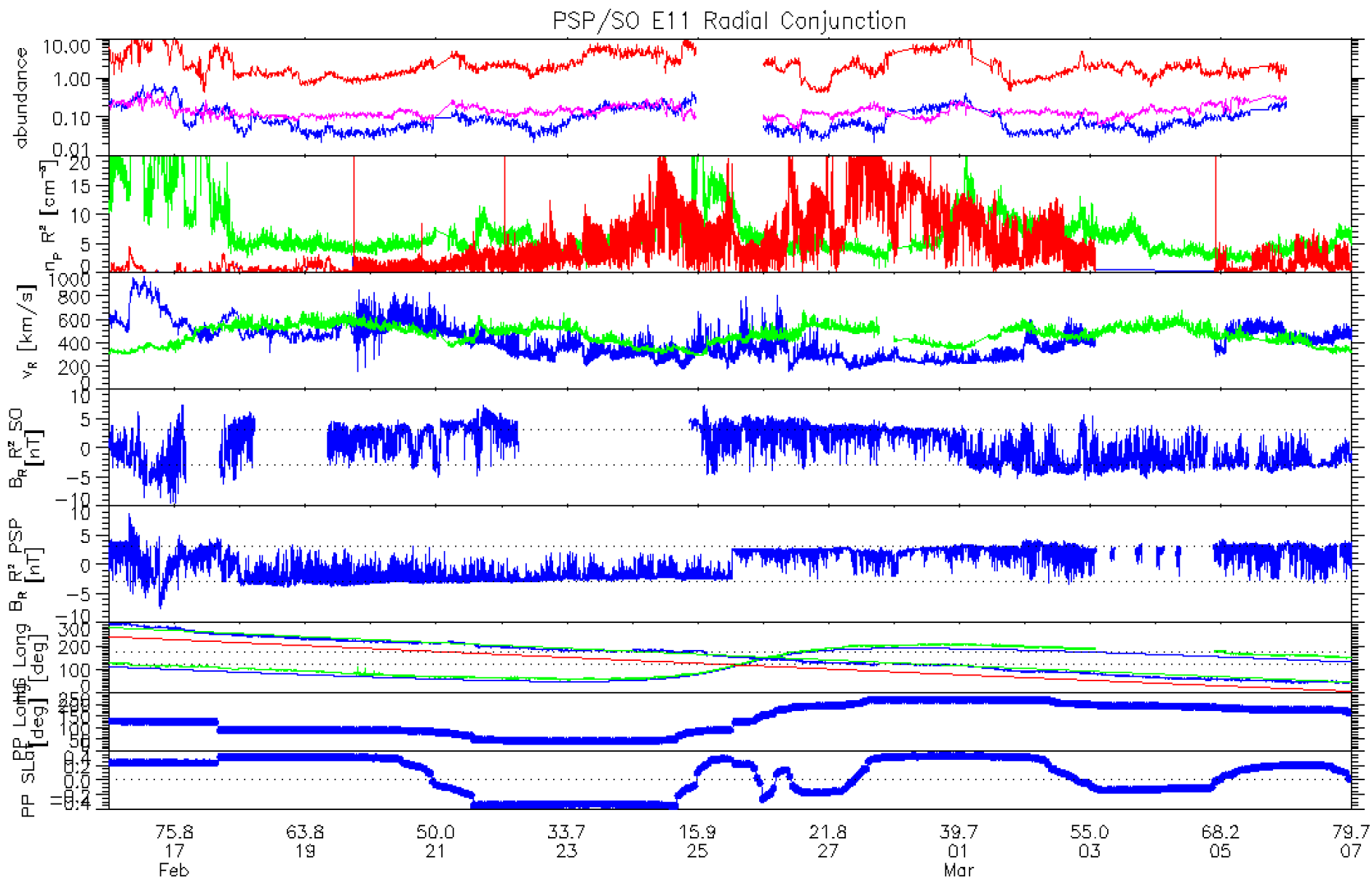
B_R * R²

B_R * R²

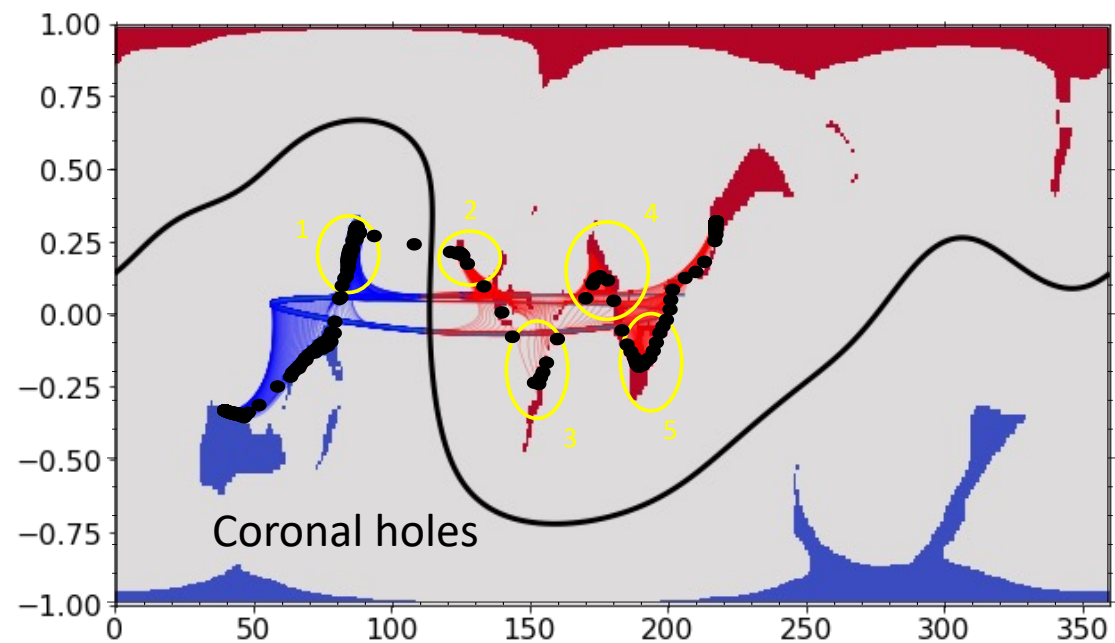
Carrington Longitude

PFSS Footpoints on Sun

Rsun
Date
2022

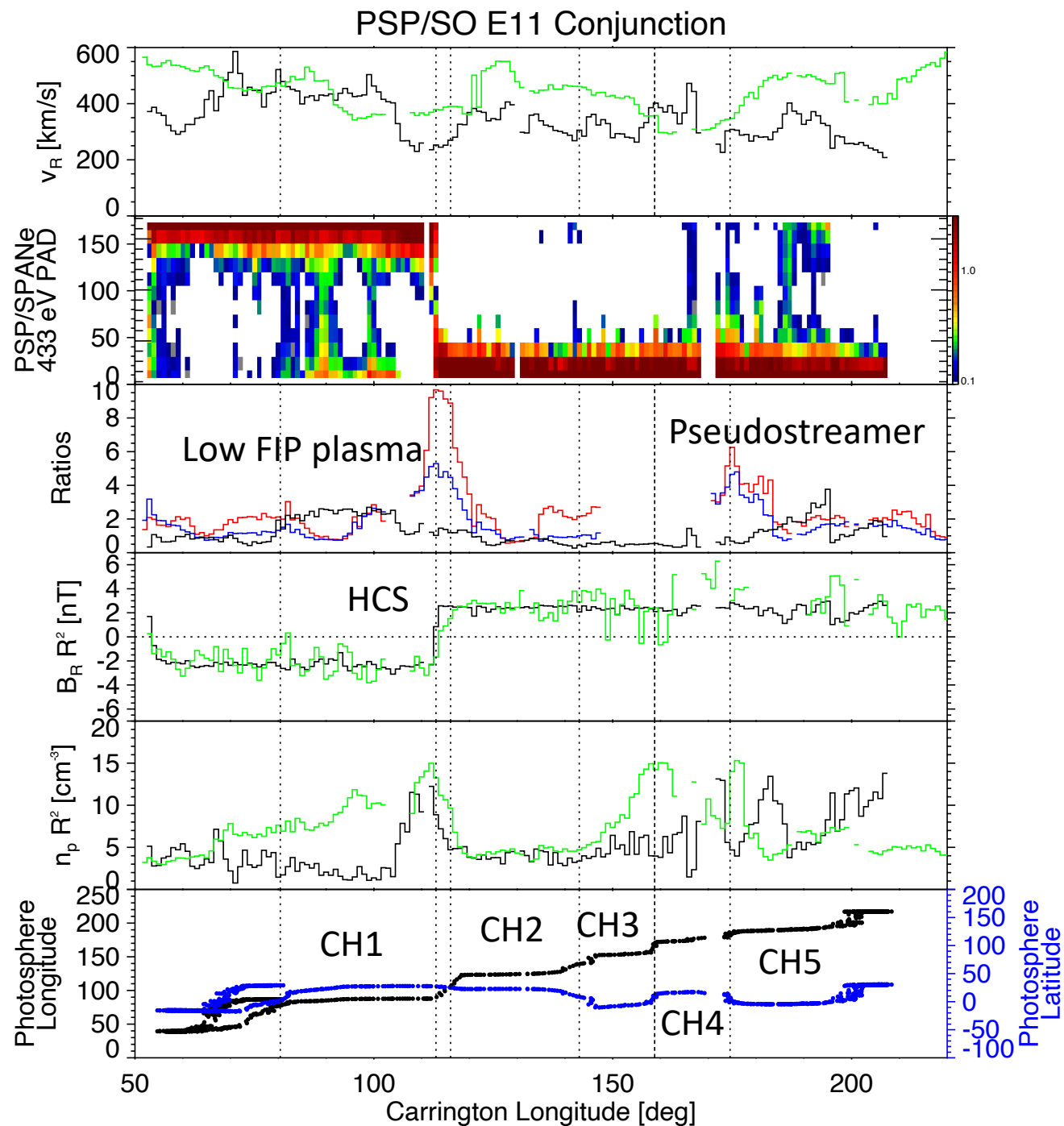


PSP and Solar Orbiter data in Carrington Coordinates



- Allows cross-platform data analysis (i.e. use SO data to study PSP phenomena)
- Radial evolution of solar wind structure

(Ervin et al., 2023)



Units and Coordinate systems

- Choose your **data analysis variables** based on the *physics* at hand, not simply on what's available out of the box
- Choose your **coordinate systems** based on the *physics* at hand, not simply on what's available out of the box